Chemie der Erde 71 (2011) 87–95

Contents lists available at ScienceDirect

Chemie der Erde

journal homepage: www.elsevier.de/chemer

# Age of the MGS5 segment of the Milanggouwan stratigraphical section and evolution of the desert environment on a kiloyear scale during the Last Interglacial in China's Salawusu River Valley: Evidence from Rb and Sr contents and ratios

Shuhuan Du[a], Baosheng Li[a,b,*], Dongfeng Niu[a], David Dian Zhang[c], Xiaohao Wen[a], Deniu Chen[d], Yi Yang[a], Fengnian Wang[a]

[a] Department of Geography, South China Normal University, Guangzhou 510631, China
[b] State Key Laboratory of Loess and Quaternary Geology, Institute of Earth Environment, Chinese Academy of Sciences, Xi'an 710061, China
[c] University of Hong Kong, Pokfulam Road, Hong Kong
[d] Institute of Zoology, Chinese Academy of Sciences, Beijing 100080, China

ARTICLE INFO

*Article history:*
Received 19 November 2009
Accepted 19 July 2010

*Keywords:*
Salawusu River Valley
Last Interglacial
MGS5 segment
Rb and Sr
Kiloyear-scale climate fluctuations

ABSTRACT

The MGS5 segment of the Milanggouwan stratigraphical section in China's Salawusu River Valley records 8.5 sedimentary cycles consisting of dune sands alternating with fluviolacustrine facies or/and paleosols. Based on a comprehensive analysis of the distribution of Rb and Sr within the segment and paleoecological evidence (fossils), it appears that the observed sedimentation cycles mainly resulted from fluctuations between dry-cold and warm-humid climates, which indicates that the MGS5 segment experienced at least eight cold-dry and nine warm-humid climatic fluctuations. Of these, 12 cold–warm climate fluctuations correspond to DO20–DO25 and stadia 21–26 recorded by the NGRIP ice cores. Another five cold–warm climatic fluctuations that occurred during MGS5e correspond to five substages (5e1–5e5) recorded by the GRIP ice cores from Greenland. This kind of high-frequency climatic fluctuation on a kiloyear scale was mainly subject to variations in the strength of the East Asian winter and summer monsoons.


## 1. Introduction

Since the 1990s, researchers from China and the abroad have obtained information on kiloyear-scale climate fluctuations during the Last Interglacial or MIS5 (marine sediments or $\delta^{18}O1$ to $\delta^{18}O5$ in continental glaciers, both of which are referred to as "MIS" hereafter) in polar ice cores (Dansgaard et al., 1993; Grootes et al., 1993; Yao et al., 1997), in ocean sediments (Wang and Yang, 1995; Tu et al., 2001; Sun and Luo, 2001), and in terrestrial sediments (An et al., 1991; Fang et al., 1996, 1999; Ren et al., 1996; Sun et al., 1996; An and Porter, 1997; Chen et al., 2000, 2003). Study of China's Luochuan Potou and Xiaheimu sections revealed the existence of nine events in which the winter monsoon strengthened during the Last Interglacial, represented by the accumulation of aeolian dust (Li et al., 1998a,b). The stalagmite records of Yuan et al. (2004) showed that the East Asian summer monsoon was weakest in subsegment 5d of MIS5, fluctuated between strengthening and declining in subsegment 5c, and remained relatively stable in subsegment 5e. Guan et al. (2007) discovered the existence of five events during MIS5 in which the summer monsoon strengthened and four events in which the winter monsoon strengthened based on their research on two sections in eastern and western Liupanshan.

During periods when the East Asian winter monsoon predominantly controls regional weather patterns, a region's climate becomes colder and drier, with increased frequency of winds capable of transporting aeolian sediments. In contrast, during periods when the East Asian summer monsoon is dominant, a region's climate becomes warmer and wetter, leading to decreased sediment transport.

The presence of high-frequency Dansgaard–Oeschger events (up to six times during the Last Interglacial) was recorded in the NGRIP ice cores (NGICP Members, 2004), which indicated a relatively stable climate during the late Eemian interglacial. Bond et al. (1993, 1997) researched the correlations between climate records from North Atlantic sediments and Greenland ice, showed that the ice cores provide evidence of North Atlantic climate changes. And these climate patterns affect the Asian monsoons (Stephen and An, 1995). Fang et al. (1996, 1999) studied the Last Interglacial loess in China's Lanzhou and Linxia areas, and found that the MIS5e exhibited three times when the East Asian summer monsoon suddenly strengthened and two times when the winter monsoon

* Corresponding author at: Department of Geography, South China Normal University, Guangzhou 510631, China. Tel.: +86 20 85214643; fax: +86 20 85217620.
*E-mail address:* libsh@scnu.edu.cn (B. Li).

0009-2819/$ – see front matter © 2010 Elsevier GmbH. All rights reserved.
doi:10.1016/j.chemer.2010.07.002

strengthened, which is similar to the five short-time-scale changes that occurred during the same period in the GRIP data.

The Salawusu River Valley, which is located on the southern margin of China's Mu Us Desert in a low-lying part of the southeastern Ordos Plateau, contains large amounts of geological information on environmental variations during the Late Quaternary. Li et al. (2000, 2005) reported the existence of kiloyear-scale climate fluctuations in the MGS5 segment that corresponded to segment MIS5 of the Last Interglacial in the Late Quaternary, and a close temporal relationship with the mainland ice-core climate data.

Based on these previous results, we chose to further examine the MGS5 segment of the Milanggouwan stratigraphical section in search of new clues to the regional paleoclimate. By determining thermoluminescence (TL) ages, in combination with proxy paleoclimatic indices (i.e., Rb and Sr contents, with reference to the grain size and magnetic susceptibility of the MGS5, and the fossil data that indicated the contemporaneous paleoecology), we attempted to understand climate variations during the Last Interglacial in the Mu Us Desert.

## 2. Study area and methods

### 2.1. The MGS5 segment

The Milanggouwan section is situated along the left bank of the middle reaches of the Salawusu River (Fig. 1), about 500 m northeast of Milanggouwan village (108°33′05.4″E, 37°45′47.2″N). The top of the profile lies at 1290 m above sea level, and the sediment thickness is about 83 m. The MGS5 stratigraphic segment is a series of sedimentary sequences with depths ranging from 36.95 to 51.93 m (Fig. 2), with a total of 24 layers from 61LS to 84S. These include 10 layers of aeolian paleo-mobile dune sands, 9 layers of fluviolacustrine facies, and 5 layers of paleosols. There is considerable overlap among the strata at different locations.

The paleo-mobile dune sands are brown-yellow (Munsell 10YR 5/8), and mainly consist of fine sands, loosely compacted and evenly sorted, with occasional plant relicts, vestiges of water currents, and ferro-rusty spots. Some layers appear to have an angle of repose typical of dune sand sediments. The fluviolacustrine facies are light greyish (2.5YR 7/2) and contain many root tissues, calcareous concretions, and ferro-rusty spots. The paleosol is brownish-drab (2.5YR 4/2) and composed of very fine sands and silts with some clay. If a dune sand and its overlying fluviolacustrine facies or/and paleosol can be taken to represent a sedimentary cycle, then these data suggest that 8.5 sedimentary cycles occurred during this stage (i.e., the bottom of segment 84S only accounts for half a cycle; Fig. 2). For convenience, we have labeled the paleo-mobile dune sands, fluvial facies, lacustrine-swamp facies, and paleosols in this paper as D, FL, LS, and S, respectively, in the names of each layer in Fig. 2.

Some fossiliferous layers are included in the stratigraphical segments: egg fragments of *Struthio* sp. in 70FD, *Coelodonta antiquitatis*

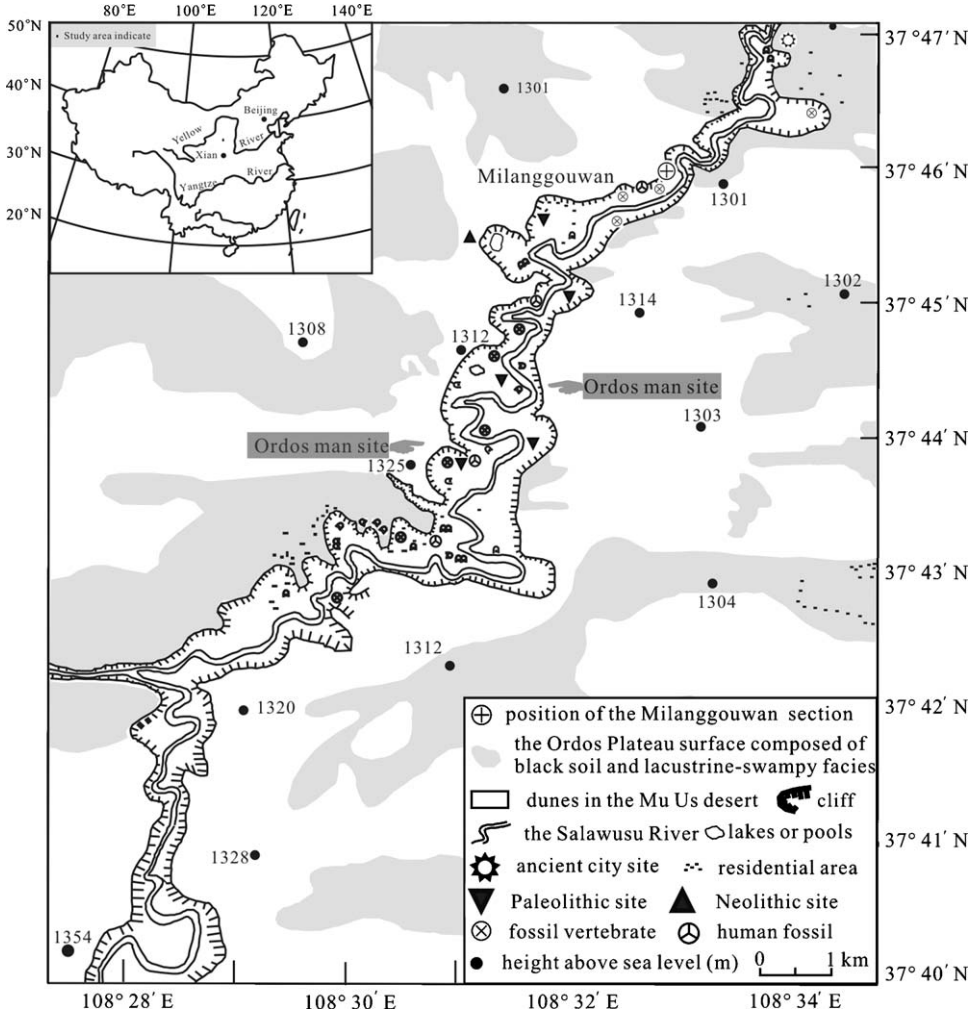


**Fig. 1.** Location and geological characteristics of the region surrounding China's Milanggouwan stratigraphical section.

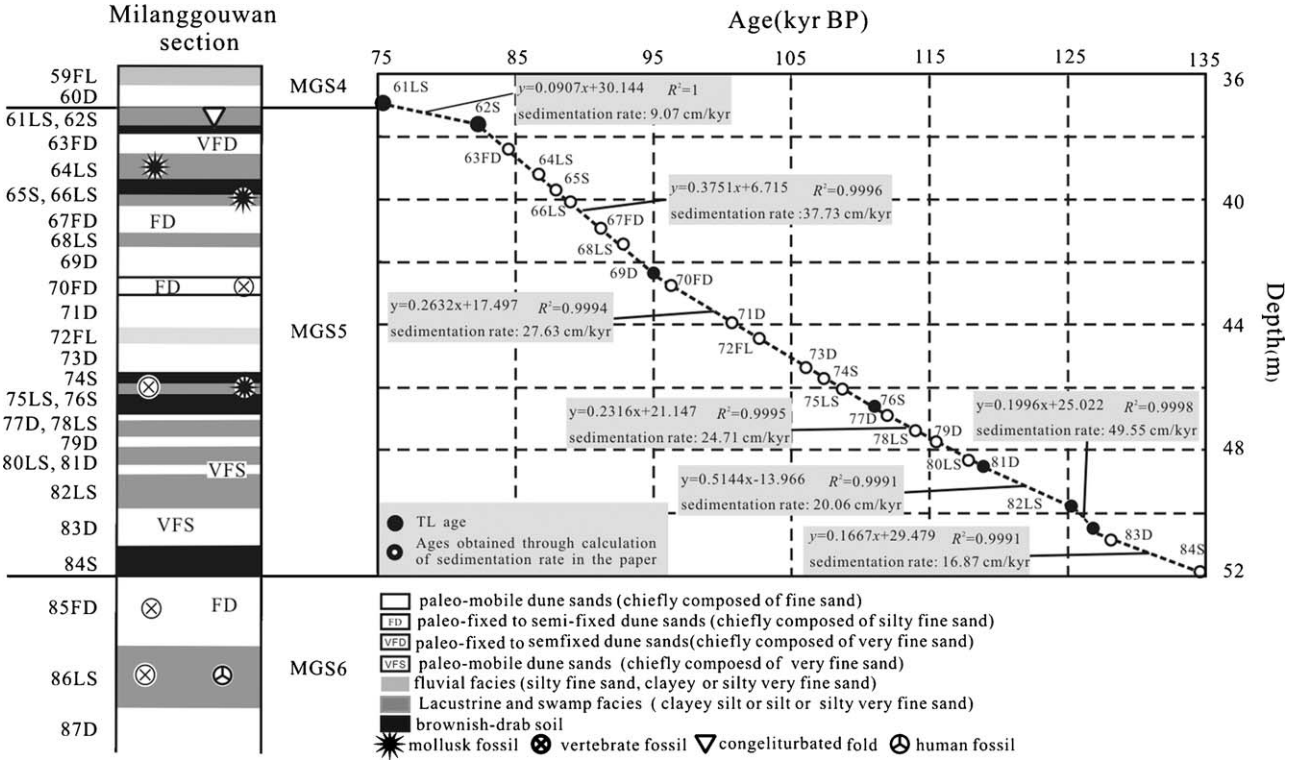


**Fig. 2.** Characteristics of the sedimentary sequences within the Milanggouwan stratigraphical section. Stratum description: D, paleo-mobile dune sands; FL, fluvial facies; LS, lacustrine-swamp facies; and S, paleosols.

in 75LS; and some fossil gastropods in 64LS and 66LS, and abundant fossil gastropods in 75LS.

### 2.2. Ages within the MGS5 segment

We dated eight layers by means of thermoluminescence (TL), including the 62S, 71FD, 76S, 81D, the central and at the top of 83D strata in MGS5, the overlying 60D stratum, and the underlying 85FD stratum. To do so, we used quartz grains smaller than 10 μm collected from the samples. The age determination was conducted by Baolin Huang and Liangcai Lu, using a Type 711 age determination instrument (Littlemore Scientific Instrument Corporation, Oxford, UK) in the TL lab of the Guangzhou Institute of Geochemistry, Chinese Academy of Sciences. The ages of each sample and the relevant parameters are listed in Table 1. Based on these ages and the depths of each section, we used linear regression to estimate the sedimentation rates during each period; the resulting equations are shown in Fig. 2.

The TL dating results show that the age at the bottom of 60D, which overlies MGS5 and belongs to MGS4, is 75.08 ± 7.40 kyr BP. This corresponds to the age of the boundary between MGS4 and MGS5, which is also the interface between 60D and 61LS. The lower limit of the sequence, at the interface between 84S and 85FD, corresponds to the boundary between MGS5 and MGS6, but there is currently no direct age data for this interface. Based on the TL dating of the strata that overly and underlie 84S, the age should be between 148 and 125 kyr BP, and with an average sedimentary rate of 16.87 cm/kyr during this period, we can estimate the interface age as 134.90 kyr BP. Thus, the ages within MGS5 are consistent with the period from 132 to 73 kyr BP in MIS5 (Martinson et al., 1987), which is usually called the "Last Interglacial".

To compare the kiloyear-scale climatic changes in the Milanggouwan section with the division scheme in the GRIP ice cores and the MIS5 marine cores, we first divided MGS5 into five stratigraphic segments based on the known TL ages and ages calculated using regression lines for sedimentation rates (Fig. 2), then we dated each segment based on different sedimentation rates. The results as follows:

MGS5a (61LS–66LS): 75.00–86.50 kyr BP
MGS5b (67FD–71D): 86.50–100.53 kyr BP
MGS 5c (72FL–76S): 100.53–111.03 kyr BP

**Table 1**
Results of the thermoluminescence (TL) dating and related parameters for strata in the MGS5 segment.

| Horizon and lab record number | Depth (m) | U (ppm) | Th (ppm) | K (%) | Annual dose (mGy) | Total dose (Gy) | TL age (kyr BP) |
|---|---|---|---|---|---|---|---|
| 60D-TGD 784 | 36.95 | 0.11 ± 0.01 | 10.06 ± 0.20 | 2.10 ± 0.02 | 2.48 ± 0.08 | 186.20 ± 13.96 | 75.08 ± 7.40 |
| 62S-TGD 785 | 37.60 | 1.07 ± 0.05 | 12.09 ± 0.24 | 2.03 ± 0.016 | 2.31 ± 0.07 | 190.00 ± 14.25 | 82.25 ± 8.50 |
| 70FD-TGD 786 | 42.75 | 0.75 ± 0.04 | 6.50 ± 0.13 | 1.99 ± 0.016 | 2.02 ± 0.06 | 193.80 ± 14.53 | 95.90 ± 9.46 |
| 76S-TGD 794 | 46.37 | 1.49 ± 0.08 | 12.29 ± 0.25 | 2.13 ± 0.017 | 2.65 ± 0.08 | 288.80 ± 23.10 | 109.00 ± 12.00 |
| 81D-TGD 787 | 48.47 | 0.42 ± 0.02 | 11.04 ± 0.22 | 1.94 ± 0.016 | 2.27 ± 0.07 | 266.76 ± 20.00 | 117.50 ± 11.70 |
| 83DT-TGD 788 | 49.74 | 1.59 ± 0.08 | 6.01 ± 0.12 | 1.97 ± 0.016 | 2.32 ± 0.07 | 287.28 ± 21.54 | 123.83 ± 12.00 |
| 83DM-XAT 601 | 50.29 | 1.50 ± 0.04 | 6.10 ± 0.15 | 1.94 ± 0.018 | 2.66 ± 0.10 | 332.27 ± 35.56 | 124.94 ± 15.84 |
| 85FD-TGD 604 | 54.18 | 0.62 ± 0.03 | 6.94 ± 0.14 | 2.42 ± 0.019 | 4.36 ± 0.13 | 646.80 ± 40.75 | 148.00 ± 12.50 |

**Table 2**
Comparison of kiloyear-scale climate events in the MGS5 segment with corresponding events in the GRIP and NGRIP data.

| Sediment cycles in the MGS5 segment | Ages of sediment cycles (kyr BP) | NGRIP | |
|---|---|---|---|
| | | Dansgaard–Oeschger and stadial data (NGICP Members, 2004) | Ages of interglacial stadia (kyr BP) (Dansgaard et al., 1993; NGICP Members, 2004) |
| 61LS, 62S | 75–83 | DO20 | 73 |
| 63FD | 83–84 | Stadial 21 | |
| 64LS, 65S, 66LS | 84–88 | DO21 | 84 |
| 67FD | 88–91 | Stadial 22 | |
| 68LS | 91–92 | DO22 | 90 |
| 69D, 70FD, 71D | 92–100 | Stadial 23 | |
| 72FL | 100–102 | DO23 | 103 |
| 73D | 102–105 | Stadial 24 | |
| 74S, 75LS, 76S | 105–110 | DO24 | 110 |
| 77D | 110–111 | Stadial 25 | |
| 78LS | 111–113 | DO25 | 115 |
| 79D | 113–114 | Stadial 26 | |
| 80LS | 114–117 | GRIP Eem 5e1 (GRIP Members, 1993) | 117.6 (Fang et al., 1999) |
| 81D | 117–118 | 5e2 | |
| 82LS | 118–122 | 5e3 | 118.6 (Fang et al., 1999) |
| 83D | 122–128 | 5e4 | |
| 84S | 128–134 | 5e5 | 123.5 (Fang et al., 1999) |

MGS5d (77D–79D): 111.03–114.44 kyr BP
MGS5e (80LS–84S): 114.44–134.90 kyr BP

Based on the results of this calculation, we calculated the age limits for each stratum by means of linear interpolation (Table 2). The results reveal 8.5 sedimentary cycles during MGS5 with fluctuations on a kiloyear-scale. On this basis, we propose an initial correspondence between each section in MGS5 and the corresponding sections in the Last Interglacial of the GRIP and NGRIP data (Table 2).

### 2.3. Data analysis

We collected and analyzed a total of 105 Rb and Sr samples at an average interval of 15 cm in the MGS5 segment of the Milanggouwan section. The analysis was performed in using an X-ray fluorescence spectrometer (Type 3070, Rigaku International Corp., Tokyo, Japan) in the Cold and Arid Regions Environment and Engineering Research Institute of Chinese Academy of Sciences. First, we dried the samples, and then ground them and sifted them through a 200-mesh screen, crushing them into smaller pieces (30 μm in diameter) to analyze. The test results were controlled by the sediment GSD9 and GSS1 of national standard, the relative deviation and the relative errors were both less than 5%.

To better illustrate the ancient environment reflected by the Rb and Sr, we also verified it by the grain size and the magnetic susceptibility in the MGS5 section. The grain size and the magnetic susceptibility value were measured in 310 samples (samples collected at an interval of 5 cm, some individuals at 3 cm or 6 cm), the Malvern Mastersizer 2000 M laser grain size analyzer (measuring range 0.02–2000 μm) was used for grain size analysis, experiment process was referred to the analysis method of loess grain size (Lu and An, 1997), and the magnetic susceptibility was measured by Bartington magnetic susceptibility instrument. The experiment is as follows: first, the sample was put in a non-magnetic polystyrene cylindrical box, 2.5 cm high with diameter of 2.2 cm, tightly pressed and weighed. Second, each sample was measured three times, and then the average value divided by the quality of the sample, thus, we got the magnetic susceptibility value.

## 3. Results and analyses

Table 3 summarizes the means and range of values for the Rb and Sr concentrations and for the Rb–Sr ratio in the five subsegments of the MGS5 segment. Table 4 summarizes the same data, but compares the three main sediment types (lithofacies) in the segment. To more clearly reveal the trends within MGS5, we have presented these data using sliding three spots averaging equally (Fig. 3). Based on these results, we can discern the following characteristics of MGS5:

(1) The Rb and Sr contents and the Rb–Sr ratios differ significantly ($P < 0.05$) among the layers, with the Rb content ranging from 47.4 to 98.2 μg/g, the Sr content ranging from 126.1 to 254.0 μg/g, and the contents averaging 72.9 and 178.4 μg/g, respectively. The Rb–Sr ratios ranged from 0.22 to 0.68, and averaged 0.41. In Fig. 3, the graph of these values over time shows considerable oscillation in the values between layers.

**Table 3**
Rb and Sr contents of samples from the MGS5 segment, and the corresponding Rb–Sr ratios during the last interglacial period, for the five subsegments shown in Fig. 2.

| Subsegments of the MGS5 segment | Rb (μg/g) | | | Sr (μg/g) | | | Rb–Sr ratio | | |
|---|---|---|---|---|---|---|---|---|---|
| | Minimum | Maximum | Average | Minimum | Maximum | Average | Minimum | Maximum | Average |
| 5a | 47.40 | 85.90 | 70.83 | 126.10 | 214.60 | 164.54 | 0.22 | 0.68 | 0.44 |
| 5b | 58.00 | 76.60 | 62.77 | 130.20 | 254.00 | 153.43 | 0.24 | 0.47 | 0.42 |
| 5c | 60.10 | 98.20 | 77.08 | 138.80 | 211.40 | 184.61 | 0.34 | 0.51 | 0.42 |
| 5d | 68.00 | 81.50 | 76.02 | 186.90 | 202.50 | 195.13 | 0.34 | 0.42 | 0.39 |
| 5e | 67.00 | 90.10 | 77.74 | 178.00 | 231.30 | 196.31 | 0.33 | 0.48 | 0.40 |

**Table 4**
Rb and Sr contents of samples from the MGS5 segment, and the corresponding Rb–Sr ratios, during the last interglacial period for the different sedimentary facies.

| Sediment type | Number of samples | Rb (μg/g) | | | Sr (μg/g) | | | Rb–Sr ratio | | |
|---|---|---|---|---|---|---|---|---|---|---|
| | | Minimum | Maximum | Average | Minimum | Maximum | Average | Minimum | Maximum | Average |
| Dune sands | 41 | 58.00 | 90.00 | 68.57 | 130.20 | 254.00 | 171.23 | 0.24 | 0.49 | 0.41 |
| Fluviolacustrine facies | 38 | 47.40 | 85.90 | 74.09 | 126.10 | 214.60 | 179.30 | 0.22 | 0.68 | 0.42 |
| Paleosols | 26 | 60.00 | 98.20 | 77.98 | 142.90 | 231.30 | 188.78 | 0.30 | 0.51 | 0.42 |

(2) The Rb and Sr contents and the Rb–Sr ratios reveal certain trends in the different subsegments. The Rb content shows obvious peaks in subsegments 5a, 5c, and 5e, but clearly lower values in subsegments 5b and 5d, and the contents averaging show peaks and lower values in the former and the latter, respectively. The Sr content shows a trend similar to that for the Rb values, but the mean contents show not significantly change in each subsegment. The Rb–Sr ratios followed trends similar to those for Rb and Sr, and were especially similar to those for Rb, but the mean ratios did not differ significantly among the subsegments; however, the Rb–Sr ratios in subsegments 5a and 5c were slightly higher than those underlying in 5b and 5d.

(3) There were obvious differences ($P < 0.05$) in the Rb and Sr contents among the different lithofacies (Table 4), with the lowest Rb and Sr contents in dune sands, the highest in paleosols, and intermediate values in fluviolacustrine facies. However, there were no significant differences in the mean Rb–Sr ratios among the lithofacies.

(4) The Rb and Sr contents appear to follow the sedimentary cycles: the Rb and Sr contents from the dune sands tend to be lower than those of the overlying fluviolacustrine or/and paleosol facies. These data suggest that the 8.5 sedimentary cycles within this section are similar to the cycles shown by the Rb and Sr data. In general, the distribution of the Rb–Sr ratios shows similar trends to those of the Rb and Sr contents; that is, the ratios increase from low in the dune sands to high in the overlying fluviolacustrine facies or/and paleosol, and this shows more obvious accumulation of Rb than of Sr after dune sands are replaced by fluviolacustrine facies or/and paleosols within a sedimentary cycle. Where differences exist, as in the cycle between 72FL and 73D, more complicated factors may explain the differences in the accumulations of Rb and Sr.

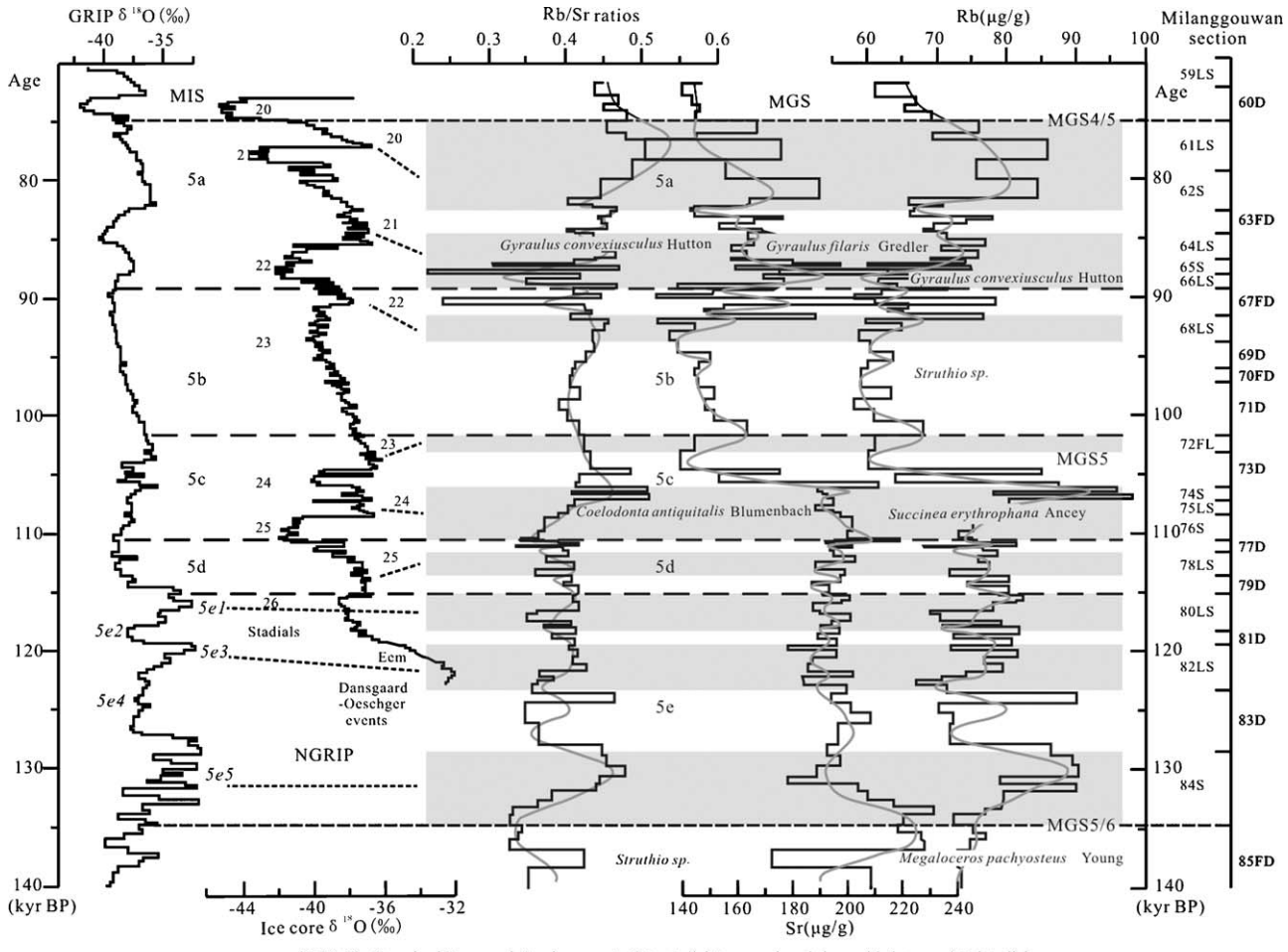


**Fig. 3.** Rb and Sr contents and Rb–Sr ratios for the five subsegments of the MGS5 segment of the Milanggouwan stratigraphical section, and comparison with results from other studies. Values for MGS5 from the present study represent three-sample moving averages.

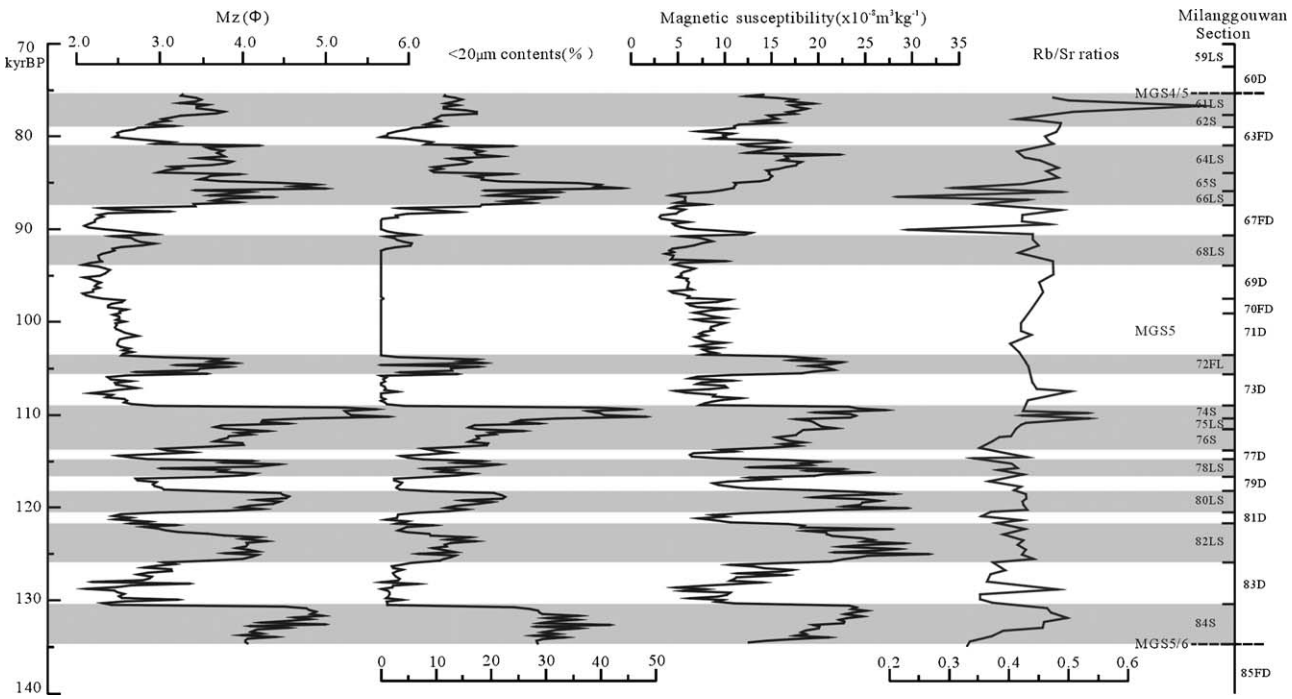


**Fig. 4.** Average grain size – *Mz*($\phi$), grain content (<20 μm), magnetic susceptibility and Rb–Sr ratios of MGS5.

Fig. 4 shows the average grain size—*Mz*($\phi$) of MGS5, magnetic susceptibility, grain content (<20 μm) and the distribution curve of Rb–Sr ratios. Among them, the average grain size was calculated by the formula developed by Folk and Ward (1957): $Mz = (\phi 16 + \phi 50 + \phi 84)/3$. The results show the *Mz* of the grain size in the MGS5 ranges from 2.07 to 5.76$\phi$, with the dune sands ranging from 2.07 to 3.66$\phi$, averaging 2.56$\phi$; the fluviolacustrine ranging from 2.07 to 4.55$\phi$, averaging 3.55$\phi$; the paleosol ranging from 2.86 to 5.76$\phi$, averaging 4.17$\phi$. Obviously, the grain size from the dune sands to the overlying fluviolacustrine or/and the paleosol appears from coarse to fine, making up a sedimentary cycle of changing thickness. The magnetic susceptibility of the MGS5 ranges from 3.04 to $31.77 \times 10^{-8}$ m$^3$ kg$^{-1}$, with the dune sands ranging from 3.04 to $19.10 \times 10^{-8}$ m$^3$ kg$^{-1}$, averaging $8.60 \times 10^{-8}$ m$^3$ kg$^{-1}$; the fluviolacustrine ranging from 3.70 to $29.46 \times 10^{-8}$ m$^3$ kg$^{-1}$, averaging $15.35 \times 10^{-8}$ m$^3$ kg$^{-1}$; the paleosol ranging from 9.54 to $31.77 \times 10^{-8}$ m$^3$ kg$^{-1}$, averaging $19.48 \times 10^{-8}$ m$^3$ kg$^{-1}$. The magnetic susceptibility values from the dune sands to the overlying fluviolacustrine or/and the paleosol appear from low to high, which simultaneously shows the changing cycle as well as *Mz*($\phi$) of the grain size, while the Rb and Sr ratios generally show the similar variation as well. In each of sediment cycle, the smaller value of *Mz*($\phi$) in the dune sands corresponds to the lower values of the magnetic susceptibility and Rb–Sr ratios. As *Mz*($\phi$) value of the overlying fluviolacustrine or/and paleosol increases, the magnetic susceptibility values and Rb–Sr ratios also increase accordingly. The content of the grain smaller than 20 μm in the MGS5 ranges from 0 to 48.26%, with the dune sands ranging from 0 to 17.97%, averaging 1.88%; the fluviolacustrine ranging from 0 to 32.53%, averaging 12.72%; the paleosol ranging from 7.70 to 48.26%, averaging 26.08%. In terms of the content distribution of the grain (<20 μ m), it seems that there is similar trend to the Rb–Sr, *Mz*($\phi$) and magnetic susceptibility changes: valley in the dune sands and peak in the overlying fluviolacustrine or/and paleosol.

Obviously, the Rb, Sr and Rb–Sr in the MGS5 indicate the similar cycles to the sedimentary facies changes, and *Mz*($\phi$), magnetic susceptibility values and the content of the grain (<20 μm) change correspondingly. Namely, they all have experienced 8.5 sedimentary cycles, the similar changes in the sedimentary facies.

## 4. Discussion

In the early 1960s, the relationship between climate and the Rb and Sr contents (especially the Rb–Sr ratios) drew much academic attention. For example, the research on various weathering rock sections by Dasch (1969) showed that Rb–Sr ratios were positively correlated with the intensity of the weathering, Rb enrichment and Sr leaching in the weathering residue were primarily up to their different activity in the weathering process. Since the late 1990s, Chinese scholars (Chen et al., 1998, 1999, 2001) have adopted Rb–Sr ratios to well indicate climatic variations during the forming periods of loess and paleosol in the Loess Plateau, suggesting that the Rb and Sr contents appeared low to high and high to low both in the loess and the overlying paleosol, respectively, which were related to the loess accumulating during winter monsoon and the following developed paleosol in the strengthening summer monsoon that resulted in Rb enrichment and Sr leaching. Thus, the Rb–Sr ratios can serve as an important indicator of the intensity of winter and summer monsoons (Pang et al., 2001). In terms of paleoclimate of the loess and paleosol in the Loess Plateau, the particle size is also an important indicator to show the strength of winter monsoon (Ding et al., 1998), while the magnetic susceptibility can serve as an indicator of the intensity of East Asian summer monsoon circulation in Chinese mainland (An et al., 1991), which is accepted by more and more scholars.

In recent years, some researchers (Wen et al., 2007; Ouyang et al., 2007; Niu et al., 2008; Ou et al., 2008) have adopted different paleoclimate indicators to analyze the sediment cycles and paleoclimate in the Milanggouwan section. The results of their studies indicate causal relationships between the alternation between dune sands and fluviolacustrine facies or/and paleosols in the geological record and cycles of cold and warm climate that reflect fluctuations in the East Asian winter and summer paleo-monsoons.

Our evaluation of the MGS5 segment of the Milanggouwan section based on the Rb and Sr contents and the Rb–Sr ratios provides confirmation of these fluctuations in the East Asian winter and summer paleo-monsoons. These data can also reveal whether climate fluctuations in the study area occurred on a kiloyear-scale during the Last Interglacial, and whether these fluctuations were similar to the Dansgaard–Oeschger events recorded in the NGRIP ice cores.

Based on these results, we propose that the low Rb contents in the MGS5b and MGS5d subsegments and the high values in the MGS5a, MGS5c, and MGS5e subsegments, supported by the corresponding changes in the Rb–Sr ratios, are evidence of periods with a strengthening East Asian winter and summer monsoons, respectively. The kiloyear-scale sediment cycles in the MGS5 segment reveal changes from low to high Rb contents and corresponding changes in the Rb–Sr ratios that indicate climate cycles in which dominance by the East Asian winter monsoon was replaced by dominance by the summer monsoon. The Salawusu River Valley and the Mu Us Desert therefore appear to have experienced 8.5 kiloyear-scale climatic cycles during the Last Interglacial. Obviously, the above-mentioned $Mz(\phi)$, magnetic susceptibility values and the content of grain (<20 μm)are the results of environment evolution of winter and summer monsoons together with Rb–Sr corresponding changes. Meanwhile, they are the strong evidence to support Rb–Sr changes indicating the climate variation.

However, the Rb and Sr contents in one sediment cycle in MGS5 do not show the same pattern of increase and decrease that is shown in the loess–paleosol records from China's Loess Plateau (Chen et al., 1998), although in both, the Rb contents increase from the dune sands to the overlying fluviolacustrine facies or/and paleosols. Moreover, both records reveal the same rate of change in the Rb–Sr ratios, which probably indicate differences between the forms of Rb and Sr movement and accumulation in the arid to semi-arid basins and low-lying lands of the present study and those in the Loess Plateau. The research of Li et al. (1998a,b) suggests that the early features of low-lying terrain had appeared in the southeastern part of the Ordos Plateau by at least 150 kyr BP, with a rugged and relatively landlocked terrain. This suggests that when the winter monsoon began strengthening during the Last Interglacial, the weather was cold and arid and the region around our study site was a likely place for strong winds and sand accumulation to occur. As a result, the Rb and Sr in the dune sand sediments were produced by mechanical erosion, transport, and accumulation processes during that period, and differences within and between periods in the Rb and Sr contents only reveal differences in the "original rock" in the source areas and in the transport process, with little chemical weathering occurring after the initial accumulation. Thus, the decrease of $Mz(\phi)$, magnetic susceptibility values and grain content (<20 μm) in the MGS5 was not accidental.

When the summer monsoon prevailed in the Last Interglacial, the study area was mainly a region in which water accumulated and strong biochemical weathering occurred. At that time, the hydrothermal conditions were better in the Salawusu River Valley and its surroundings, and both the low-lying lands and surrounding terrain above the normal river level (such as the valley slopes and islands above the water surfaces that formed in low-lying lands) were mainly subject to the influence of biochemical weathering. Subsequently, much of the Sr was leached out of the surface sediments and concentrated at the bottom of the low-lying lands, whereas much of the Rb accumulated in higher terrain because this element is more resistant to leaching. In the higher terrain where Rb accumulated before being influenced by strong precipitation, Rb followed the movement of water, moving towards low-lying terrain and mixing with the Sr. Meanwhile, biochemical weathering was continuously renewing the processes described above for higher terrain, with Sr continuously leaching and much new Rb becoming concentrated in this terrain before moving downwards into the low-lying terrain during the next period of strong precipitation.

As a result of these processes during the prevailing summer monsoon on a kiloyear-scale period, weathering leading to the accumulation of Rb and leaching of Sr followed by the erosion of Rb and accumulation of both Rb and Sr repeated, thereby increasing both the Rb and Sr contents in the fluviolacustrine facies compared with their values in the underlying sediments. Another inevitable phenomenon would be increases of the Sr content in brown-drab soils compared with the values in the underlying dune sands. In theory, aerobic weathering and soil formation processes lead to Rb accumulation and Sr leaching, but we found sediment cycles of paleosols in the MGS5 segment in which the Sr content was usually higher than that of the underlying dune sands (Fig. 3). For example, the mean Sr content in 76S was 204.55 μg/g, which is higher than the value of 195.73 μg/g in the underlying 77D, probably caused by the low-lying lands of the paleosol development at that time. At the same time, increasing precipitation triggered a rising water table, resulting in percolation of belowground water with a relatively high Sr content into the paleosol.

In addition, the Rb–Sr ratios were abnormal in some sediment cycles. For example, the Rb–Sr ratio in 72FL (0.42) was lower than that in the underlying 73D (0.44), but the Rb and Sr contents in 72FL were both higher than those in 73D (Rb: 68.00 μg/g, 1 sample, 67.55 μg/g, the average of 4 samples; Sr: 163.00 μg/g, 1 sample, 152.68 μg/g, the average of 4 samples, respectively). The greater accumulation of Sr than of Rb may have resulted from strong leaching of Sr from areas above the water surface and the resulting greater recharge of Sr by leaching compared with the recharge of Rb by percolating water. It is interesting that this so-called abnormal situation of Rb–Sr ratios appeared in the sediments of a closed lake basin in Inner Mongolia-Daihai (40°28′07″–40°39′06″N, 112°32′31″–112°48′40″E). According to the study of recent 500 year-lake core in this place, Jin et al. (2001) suggested that Rb–Sr ratios primarily depended on the content changes of Sr in the closed lake environment. During the dry and cold period, Sr is restrained from the host rock, Rb–Sr ratios increase, while in the warm and wet period, it is easy for Sr to leach, Rb–Sr ratios decrease. In this sense, the abnormal of Rb–Sr ratios reflected in the 72FL–73D cycle perhaps related to the water in the closed environment during 72FL period as well.

Significantly, the peaks and low values for Rb content and the Rb–Sr ratio correspond well to the paleoecology, as indicated by fossils found in the MGS5 segment. For example, the Rb content and Rb–Sr ratio in 70FD are accompanied by the presence of fossil fragments of the eggs of *Struthio* sp., which indicate the presence of a cold and arid desert environment. Conversely, rising Rb contents and Rb–Sr ratios in 64LS, 66LS, and 75LS, which contained gastropods fossils (Table 5), indicate the presence of a warm-moist climate. In particular, the large number of *Gyraulus convexiusculus*

**Table 5**
Mollusk fossils found in the lacustrine facies from the last interglacial period in the Milanggouwan section.

| Fossils | Horizons | | |
|---|---|---|---|
| | 64LS | 66LS | 75LS |
| *Gyraulus convexiusculus* **Hutton** | + | + | + |
| *Gyraulus filaris* **Gredler** | + | – | – |
| *Succinea erythrophana* **Ancey** | – | – | + |
| *Radix cucunorica* **Mollendorff** | – | – | + |
| *Polypylis hemisphaerula* **Benson** | – | – | + |
| *Galba pervia* **Martens** | + | – | + |
| *Sucinea evoluta* **Martens** | – | – | + |
| *Vallonia patens* **Reinhardt** | + | – | – |
| *Vallonia* **sp.** | + | – | – |
| *Succinea* **sp.** | – | + | – |
| *Pisidium* **sp.** | – | – | + |

fossils in 75LS probably indicates a warm-temperate zone (possibly even a sub-tropical zone) with a warmer and more humid climate. Modern Chinese species in this group of organisms mainly inhabit the Jiangsu, Zhejiang, Fujian, Taiwan, Guangdong, Guangxi, and Yunnan regions, where they live in warm water, and their northernmost distribution is near Nanniwan (109°39′E, 36°19′N), which represents the boundary of the warm-temperate zone near Yan'an, in Shannxi Province. Other significant indicators of a warm-humid climate included the presence of the terrestrial snail *Succinea erythrophana* and the aquatic snail *Galba pervia*; although modern individuals of these species are widespread in both southern and northern China, they are more abundant in the Yangtze River basin and in the Guangdong area of Guangxi province, both of which are warm and humid. These fossil data therefore support the relationship between the observed variations in Rb contents and Rb–Sr ratios and fluctuations in the East Asian winter and summer monsoons.

The results of our study support the conclusion that 8.5 climate cycles were revealed by the variations in Rb and Sr contents and in the Rb–Sr ratio in the MGS5 segment, and that these cycles represent kiloyear-scale fluctuations in the East Asian winter and summer monsoons during the Last Interglacial in the Mu Us Desert. Consequently, during this period, we propose that there were eight periods dominated by the winter monsoon and nine dominated by the summer monsoon. The ages of the layers that were most strongly influenced by the winter monsoon are 83–84 kyr BP for 63FD, 88–91 kyr BP for 67FD, 92–100 kyr BP for 69D plus 70FD plus 71D, 102–105 kyr BP for 73D, 110–111 kyr BP for 77D, 113–114 kyr BP for 79D, 117–118 kyr BP for 81D, and 122–128 kyr BP for 83D. The ages of the layers that were most strongly influenced by the summer monsoon are 75–83 kyr BP for 61LS plus 62S, 84–88 kyr BP for 64LS plus 65S plus 66LS, 91–92 kyr BP for 68LS, 100–102 kyr BP for 72FL, 105–110 kyr BP for 74S plus 75LS plus 76S, 111–113 kyr BP for 78LS, 114–117 kyr BP for 80LS, 118–122 kyr BP for 82LS, and 128–134 kyr BP for 84S (Table 2).

The time sequence of the variations in the East Asian winter and summer monsoons, as indicated by the Rb and Sr contents and the Rb–Sr ratios in the MGS5 segment, correlate well with the Dansgaard–Oeschger climate variations recorded by the ice-core oxygen isotope contents at high latitudes. Occurrence of Dansgaard–Oeschger cycles were attributed to the changes of thermohaline circulation (THC) according which the melt water with less salinity prevented the formation of North Atlantic Deep Water, then THC was weakened, sometimes even shut down completely. This reduced greatly the transportation of heat to the North Atlantic (Clark et al., 1999). During this period, stadials and Last Glacial Maximum appeared. That was also the East Asian winter monsoon predominantly controls China (An, 2000). Once the NADW recovered, the THC intensified again. And led to the interstadials and interglacial occurred. Then the East Asian summer monsoon was dominant. The layers that mainly formed under the influence of the summer monsoon (61LS + 62S, 64LS + 65S + 66LS, 68LS, 72FL, 74S + 75LS + 76S, and 78LS) correspond to the DO20–DO25 sequence recorded by the NGRIP ice cores; 63FD, 67FD, 69D + 70FD + 71D, 73D, 77D, and 79D correspond to the stadia 21–26 sequence of the NGRIP ice cores. The MGS5e subsegment (80LS–84S) is equivalent to the 5e subsegment of the GRIP ice cores. Three peaks (80LS, 82LS, and 84LS) separated by two lower values (81D and 83D), revealed by the Rb and Sr contents and the Rb–Sr ratios, also correspond well to three peaks separated by two lower values (5e1–5e5; Fig. 3) in the oxygen isotope curve. This suggests that the movement and accumulation of Rb and Sr in the Salawusu River Valley or the Mu Us Desert during the Last Interglacial were governed by fluctuations in the East Asian winter and summer monsoons, which were in turn caused by the North Atlantic thermohaline circulation.

## Acknowledgments

This paper funded by National Basic Research Program of China, Grant Number: 2010CB833405, 2004CB720206; National Natural Science Foundation of China, Grant Number: 40772118, 49971009; Research Grants Council Grant of the Hong Kong Special Administrative Region, Grant Number: HKU 7243/04H. We thank Jingzhao Zhan (Institute of Earth Environment, Chinese Academy of Sciences) and Liangcai Lu (Heat Releasing Optics Laboratory, Earth Chemistry Research Institute, Chinese Academy of Sciences) for their determination of the TL ages. We are grateful to Geoff Hart for his thorough review that has improved the manuscript substantially.

## References

An, Z.S., 2000. The history and variability of the East Asian paleomonsoon climate. Quaternary Science Reviews 19, 171–187.
An, Z.S., Porter, S.C., 1997. Millennial-scale climatic oscillations during the last interglaciation in central China. Geology 25, 603–606.
An, Z.S., Wu, X.H., Wang, P.X., Wang, S.M., Dong, G.R., Sun, X.J., Zhang, D.E., Lu, Y.S., Zheng, S.H., Zhao, S.L., 1991. Paleomonsoons of China over the last 130,000 years – paleomonsoon records. Science in China (Series B): Chemistry 34, 1007–1015.
Bond, G., Broecker, W., Johnson, S., Jouzel, J., Labeyrie, L., McManus, J., Bonani, G., 1993. Correlations between climate records from North Atlantic sediments and Greenland ice. Nature 365, 143–147.
Bond, G., Showers, W., Cheseby, M., Lotti, R., Almasi, P., deMenocal, P., Priore, P., Cullen, H., Hajdas, I., Bonani, G., 1997. A pervasive millennial-scale cycle in north Atlantic Holocene and glacial climates. Science 278, 1257–1266.
Chen, F.H., Feng, Z.D., Zhang, J.W., 2000. Loess particle size data indicative of stable winter monsoon during the last interglacial in the western part of the Chinese Loess Plateau. Catena 39, 233–244.
Chen, F.H., Qiang, M.R., Feng, Z.D., Wang, H.B., Bloemendal, J., 2003. Stable East Asian monsoon climate during the Last Interglacial (Eemian) indicated by paleosol S1 in the western part of the Chinese Loess Plateau. Global and Planetary Change 36, 171–179.
Chen, J., An, Z.S., Wang, Y.J., Ji, J.F., Chen, C., Lu, H.Y., 1998. Distribution of Rb and Sr in the Luochuan loess–paleosol sequence of China during the last 800 ka—implications for paleomonsoon variations. Science in China (Series D): Earth Sciences 41, 235–241.
Chen, J., Wang, Y.J., Chen, C., Liu, L.W., Ji, J.F., Lu, H.Y., 2001. Rb and Sr geochemical characterization of the Chinese Loess and its implications for palaeomonsoon climate. Acta Geologica Sinica 75, 259–266 (in Chinese with English summary).
Chen, J., Wang, Y.J., Ji, J.F., Chen, C., Lu, H.Y., 1999. Rb–Sr variations and its climatic stratigraphical significance of a loess-paleosol profile from Luochuan, Shaanxi province. Quaternary Sciences 7, 350–356 (in Chinese with English summary).
Clark, P.U., Webb, R.S., Keigwin, L.D., 1999. Mechanisms of global climate change at millennial time scales. Geophysical Monograph Series 112, 394.
Dansgaard, W., Johnsen, S.J., Clausen, H.B., Dahl-Jensen, D., Gundestrup, N.S., Hammer, C.U., Hvidberg, C.S., Steffensen, J.P., Sveinbjrnsdőttir, A.E., Jouzel, J., Bond, G.C., 1993. Evidence for general instability of past climate from a 250-kyr ice-core record. Nature 364, 218–220.
Dasch, E.J., 1969. Strontium isotopes in weathering profiles, deep sea sediments and sedimentary rocks. Geochimica et Cosmochimica Acta 33, 1521–1552.
Ding, Z.L., Sun, J.M., Yu, Z.W., Liu, D.S., 1998. Chronology of environmental events over East-Asia during the past 130 ka. Chinese Science Bulletin 43, 1761–1770.
Fang, X.M., Banerjee, S.K., Li, J.J., Dai, X.R., Guang, D.H., 1999. Environmental and rock magnetic studies of rapid fluctuations of Asian summer monsoon during the last interglacial maximum (MIS 5e). Chinese Science Bulletin 44, 952–954.
Fang, X.M., Dai, X.R., Li, J.J., Cao, J.X., Guang, D.H., Hao, Y.P., Wang, J.L., Wang, J.M., 1996. Abruptness and instability of Asian Monsoon—an example from soil genesis during the last interglacial. Science in China (Series D): Earth Sciences 26, 154–160 (in Chinese with English summary).
Folk, P.L., Ward, W.D., 1957. Brazos Reviver bar: a study in the significance of grain size parameters. Journal of Sedimentary Petrology 27, 3–26.
GRIP Members, 1993. Climate instability during the last interglacial period recorded in the GRIP ice core. Nature 364, 203–207.
Grootes, P.M., Stulver, M., White, W.C., Johnsen, S.J., Jouzel, J., 1993. Comparison of oxygen isotope records form the GISP2 and GRIP Greenland ice cores. Nature 366, 552–554.
Guan, Q.Y., Pan, B.T., Gao, H.S., Li, P.Y., Wang, J.P., Su, H., 2007. Instability characteristics of the East Asian Monsoon recorded by high-resolution loess sections from the last interglacial (MIS5). Science in China (Series D): Earth Sciences 50, 1067–1075.
Jin, Z.D., Wang, S.M., Shen, J., Zhang, E.L., Ji, J.F., Li, F.C., 2001. Weak chemical weathering during the Little Ice Age recorded by lake sediments. Science in China (Series D): Earth Sciences 44, 652–658.
Li, B.S., David, D.Z., Jin, H.L., Wu, Z., Yan, M.C., Sun, W., Zhu, Y.Z., Sun, D.H., 2000. Paleo-monsoon activities of Mu Us Desert, China since 150 ka B. P.—a study of the stratigraphic sequences of the Milanggouwan Section, Salawusu River area. Palaeogeography, Palaeoclimatology, Palaeoecology 162, 1–16.

Li, B.S., Jin, H.L., Lv, H.Y., Zhu, Y.Z., Dong, G.R., Sun, D.H., Zhang, J.K., Gao, Q.Z., Yan, M.C., 1998a. Processes of the deposition and vicissitude of Mu Us Desert, China since 150 ka B.P. Science in China (Series D): Earth Sciences 41, 248–254.

Li, B.S., Zhang, D.D., Wen, X.H., Dong, Y.X., Zhu, Y.Z., Jin, H.L., 2005. A multi-cycle climatic fluctuation record of the last interglacial period: typical stratigraphic section in the Salawusu River Valley on the Ordos Plateau, China. Acta Geologica Sinica 79, 398–404.

Li, L., Sun, Y.B., Lu, H.Y., Lai, Z.P., An, Z.S., 1998b. Comparison between dust events during the last interglacial in Chinese Loess Plateau and the cold events in the North Atlantic. Chinese Science Bulletin 43, 90–93 (in Chinese with English summary).

Lu, H.Y., An, Z.S., 1997. The experiment impact study of the pre-treatment methods on loess sediment grain size measurement. Chinese Science Bulletin 42, 2535–2538.

Martinson, D.G., Pisias, N.G., Hays, J.D., Imbrie, J., Moore, T.C., Shackleton, 1987. Age dating and the orbital theory of the ice ages: development of a high-resolution 0 to 300,000a-year chronostratigraphy. Quaternary Research 27, 1–29.

NGICP Members, 2004. High-resolution record of Northern Hemisphere climate extending into the last interglacial period. Nature 431, 147–151.

Niu, D.F., Li, B.S., Du, S.H., Wen, X.H., Qiu, S.F., Ou, X.J., Yang, Y., 2008. Cold events of Holocene indicated by primary elements distribution of the high-resolution sand dunes in the Salawusu River Valley. Journal of Geographical Sciences 18, 26–36.

Ou, X.J., Li, B.S., Jin, H.L., Dong, G.R., Zhang, D.D., Wu, Z., Wen, X.H., Zeng, L.H., Ouyang, C.T., Yang, Y., Liu, Y.F., 2008. Sedimentary characteristics of paleo-eolian dune sands Salawusu Formation of the Salawusu River Valley. Acta Geographica Sinica 18, 211–224.

Ouyang, C.T., Li, B.S., Ou, X.J., Wen, X.H., Zeng, L.H., Yang, Y., Liu, Y.F., 2007. Chemical weathering of the Milanggouwan paleosols in the Salawusu River Valley and their paleoclimatic implication during the last interglacial period. Acta Geographica Sinica 62, 518–528 (in Chinese with English summary).

Pang, J.L., Huang, C.C., Zhang, Z.P., 2001. Rb, Sr elements and high resolution climatic records in the Loess-Paleosol profile at Qishan, Shannx. Acta Sedimentologica Sinica 19, 637–641 (in Chinese with English summary).

Ren, J.Z., Ding, Z.L., Liu, T.S., Sun, J.M., Zhou, X.Q., 1996. Climatic changes on millennial time scale—evidence from a high-resolution loess record. Science in China (Series D): Earth Sciences 39, 449–459.

Stephen, C.P., An, Z.S., 1995. Correlation between climate events in the North Atlantic and China during the last glaciation. Nature 375, 305–308.

Sun, D.H., Wu, X.H., Liu, T.S., 1996. Evolution of the summer monsoon regime over the Loess Plateau of the last 150 ka. Science in China (Series D): Earth Sciences 9, 503–511.

Sun, X.J., Luo, Y.L., 2001. Pollen record of the last 280 ka from deep sea sediments of the northern South China Sea. Science in China (Series D): Earth Sciences 44, 879–888.

Tu, X., Zheng, F., Wang, J.L., Cai, H.M., Wang, P.X., Bühring, C., Sarnthein, M., 2001. An abrupt cooling event early in the last interglacial in the northern South China Sea. Science in China (Series D): Earth Sciences 44, 865–870.

Wang, J., Yang, H., 1995. Transfer function and the depth changes of the South Yellow Sea (China) in the last 130,000 years. Scientia Geographica Sinica 15, 321–326 (in Chinese with English summary).

Wen, X.H., Li, B.S., Zhang, D.D., Qiu, S.F., Ye, J.P., Du, S.H., Guo, Y.H., Chen, D.N., 2007. Megainterstadial climate of the Salawusu Valley-Milanggouwan stratigraphical section. Acta Geologica Sinica 81, 553–561 (in Chinese with English summary).

Yao, T.D., Thompson, L.G., Shi, Y.F., Qin, D.H., Jiao, K.Q., Yang, Z.H., Tian, L.D., Thompson, E.M., 1997. Climate variation since the last interglaciation recorded in the Guliya ice core. Science in China (Series D): Earth Sciences 40, 662–668.

Yuan, D.X., Cheng, H., Edwards, R.L., Carolyn, A.D., Megan, J.K., Zhang, M.L., Qing, J.M., Lin, Y.S., Wang, Y.J., Wu, J.Y., Jeffery, A.D., An, Z.S., Cai, Y.J., 2004. Timing, duration, and transitions of the last interglacial Asian monsoon. Science 304, 575–578.